

## Design and implementation of 4-quadrant chopper for speed control of EVs and regenerative braking analysis

Magdy Saoudi Abdelfatah<sup>1,2</sup>, Parmal Singh Solanki<sup>1</sup>, Sasidharan Sreedharan<sup>1</sup>

<sup>1</sup>Electrical Engineering Unit, Department of Engineering, University of Technology and Applied Sciences, Suhar, Oman

<sup>2</sup>Electrical Power and Machines Engineering Department, Zagazig University, Zagazig, Egypt

### Article Info

#### Article history:

Received Dec 10, 2023

Revised Nov 8, 2024

Accepted Dec 26, 2024

#### Keywords:

4-quadrant chopper

DC motor

Electric vehicles

Pulse-width modulation

Regenerative braking

### ABSTRACT

This paper presents a novel 4-quadrant chopper design for controlling the speed of electric vehicles, featuring a regenerative braking mechanism to improve energy efficiency. Regenerative braking recovers energy during deceleration by converting kinetic energy into electrical energy stored in the battery. This process activates automatically when the accelerator pedal is released, slowing the vehicle while reducing reliance on mechanical brakes, which remain available for emergency situations. The system's voltage control is achieved using a pulse-width modulation (PWM) technique that adjusts the duty cycle of switching devices. A microcontroller serves as the system's core, generating PWM signals and coordinating its operation. The performance of the chopper was evaluated through simulations and experiments, demonstrating that optimal energy recovery occurs at duty cycles of 55-65%. The results revealed that up to 400 joules of energy can be regenerated per braking cycle, particularly in stop-start driving conditions. This innovative design contributes to a 5-10% extension in battery life per charge cycle, enhancing the overall efficiency and sustainability of electric vehicles. The proposed system demonstrates significant potential for energy recovery and reduced wear on mechanical braking systems, paving the way for more efficient electric vehicle technologies.

*This is an open access article under the [CC BY-SA](#) license.*



### Corresponding Author:

Magdy Saoudi Abdelfatah

Electrical Engineering Unit, Department of Engineering, University of Technology and Applied Sciences  
Suhar Campus, Suhar, P.O. Box 135, Postal Code 311, Oman

Email: magdy.saoudi@utas.edu.om

## 1. INTRODUCTION

The most of conventional passenger and transportation vehicles across the world are operated by the fossil fuel based internal combustion engines. These vehicles are major contributors of producing the greenhouse gases other pollutants [1]-[3]. Therefore, it is essential to shift the paradigm of conventional vehicle by electric vehicles (EVs) with no tailpipe in phased manner. The various studies show that EVs are more efficient, smarter, and environmentally friendly [4]-[6]. But the range (distance covered by vehicle when fully charged) of EVs is major challenge because of limited stored energy in the battery bank. To address this issue several studies have been done to improve the EV range. In literature [7]-[9], different methods have been reported to increase EV's range and its economy. The power train of an EV classically consists of an energy source, an electric circuit (power electronics), electronic control unit (ECU), and an electric motor.

Since battery pack is the primary energy source to operate the DC motors of EVs, special attention has been given to keep the battery charge high as good lasting source and opting for newer, highly efficient designed motors. The four-quadrant DC-DC choppers, as shown in section 2, attempts to harvest a variable DC voltage from a constant DC voltage by adjusting the voltage and current passage in the four-quadrant

functions. Several studies show [10]-[12], that the use of brushless DC (BLDC) motors controlled by DC chopper is one of options to improve the performance of EVs and consumed lesser energy. In a DC chopper, DC to DC converter is used to step up and step down the DC voltage using fast operating switches. The output voltage of chopper circuit is controlled by periodic closing and opening of semiconductor switches like power transistors or forced commutation thyristors used in the circuit. The DC chopper is capable to operate in all 4-quadrants and it is more efficient, speedy and optimized device hence is widely used as speed controller for DC motors' applications [13], [14] like in EVs.

In present scenario to reduce the carbon emissions and to address the climate change issues, solar energy optimization in distributed system [15] and the use of EVs are getting priorities to replace the conventional power and transportation system respectively. There are several challenges which needs to be address for EVs like range anxiety, charging infrastructure, charging speed and compatibility [16], [17]. One of the major challenges in EVs is to increase the driving range in one charge of the battery. The performance of battery depends on many factors and scientists are developing better battery technology to increase driving range while reducing weight, cost and charging time. The other way to prolong the EV range is to recover the energy already spent. That is the known as the regeneration. For instance, incorporating a regenerative braking system over conventional friction braking during the retardation period of the wheels also has been testified in several studies to increase the driving range [18]-[23]. Many scholars are explaining the energy savings by DC chopper circuits for EVs, but little contribution has come across to find out the optimum duty cycle for regenerative braking. The objective of the work is to simulate the 4-quadrant chopper to determine the optimized range of duty cycle to get energy back during braking to charge the battery.

In this paper the design and implementation of 4-quadrant chopper to control the DC motors for electric vehicles has been discussed. Further to improve the energy efficiency, the concept of regenerative braking has been analyzed using simulations. The paper is consisting of four major sections. The background of chopper circuit, DC motors, and the need of regenerative braking has been discussed in section 1. The methodology to implement the 4-quadrant chopper and the regenerative braking has described in section 2. The section 3 presents the hardware implementation, the obtained experimental and simulation results. Finally, the conclusions are listed in the section 4.

## 2. METHODOLOGY

In regenerative mode of operation, the motor operate as generator and the kinetic energy of motor and inertia of the vehicle is converted into centricity to decrease the speed of the motor and returned power to charge the battery to save its energy and to enhance the performance of driving range [24], [25]. The 4-quadrant choppers plays vital role to control the mode of operation of the motor.

### 2.1. 4-Quadrant chopper operation

To design the different quadrants chopper, several studies has been carried out by the scholars [26]-[29] and one such chopper circuit is shown in Figure 1. It can operate in all 4-quadrants of the output voltage and current plane and is also known as a class-E chopper. The circuit of a 4-quadrant chopper consists of four power semiconductor switches. These devices used for a chopper circuit can be forced commutated thyristors, power BJTs, power MOSFETs, GTOs, or IGBTs, as shown in Figure 1. Each device has an antiparallel diode built inside or connected outside. The switches are turned on and off using pulse width modulation signals.

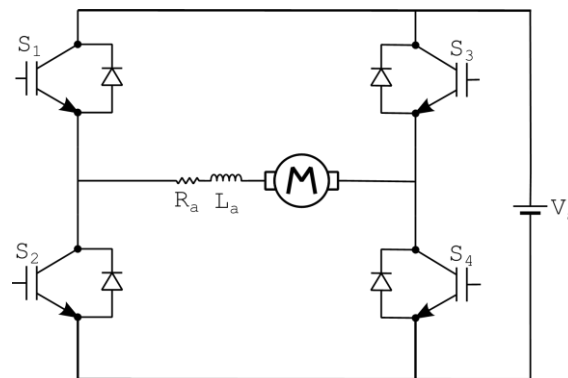


Figure 1. Four-quadrant chopper schematic diagram

The operation of a class-E chopper in all four quadrants is achieved by turning on different switches and diodes in pairs of various combinations. To obtain first quadrant operation as shown in Figure 2, PWM signal is applied in  $S_1$ ,  $S_3$  is fully OFF,  $S_4$  is fully ON, and  $S_2$  is OFF or with PWM complement to the PWM applied in upper transistor  $S_1$ , both the output voltage and current should be positive. In this mode, the motor works in the motoring mode. The developed torque and speed are positive, and the motor rotates in a certain direction, for example, clockwise direction, in Figure 2(a) the PWM is high for the transistor  $S_1$ , so the current flows through the upper transistor to the motor and transistor  $S_4$ . Now, the speed of the motor can be varied by varying the duty cycle of the transistor  $S_1$ . As the duty cycle varies, the voltage across the armature of the motor varies proportionally, thereby varying the motor speed since  $N$  is proportional to the armature voltage. In Figure 2(b) the PWM is low for the transistor  $S_1$ , so the current circulates through the diode antiparallel to the lower transistor  $S_2$ . The motor works in the forward motoring mode.

To obtain second quadrant operation, as shown in Figure 3, PWM signal is applied to  $S_2$ ,  $S_4$  is fully ON, and  $S_1$  and  $S_3$  are fully OFF. The output voltage is positive, but the current is negative. In this mode, the motor works in the forward regenerative braking mode, and the developed torque is negative, causing the machine to slow down. However, the motor still rotates in the same direction due to inertia. In Figure 3(a), the PWM is high for the transistor  $S_2$ , so the current flows through the lower transistor  $S_2$ , and the motor armature coil stores kinetic energy. Once the PWM signal is low for the transistor  $S_2$ , the stored energy returns to the supply through the diode antiparallel to transistor  $S_1$  as shown in Figure 3(b).

To obtain third quadrant operation as shown in Figures 4(a) and 4(b), PWM signal is applied to  $S_3$ ,  $S_1$  is fully OFF,  $S_2$  is fully ON, and  $S_4$  is OFF or with PWM complement to the PWM applied in upper transistor  $S_3$ . The motor rotates in counter clockwise direction. The motor works in the reverse motoring mode. To obtain fourth quadrant operation, as shown in Figures 5(a) and 5(b), PWM signal is applied to  $S_4$ ,  $S_2$  is fully ON, and  $S_1$  and  $S_3$  are fully OFF. The motor works in the reverse regenerative braking mode.

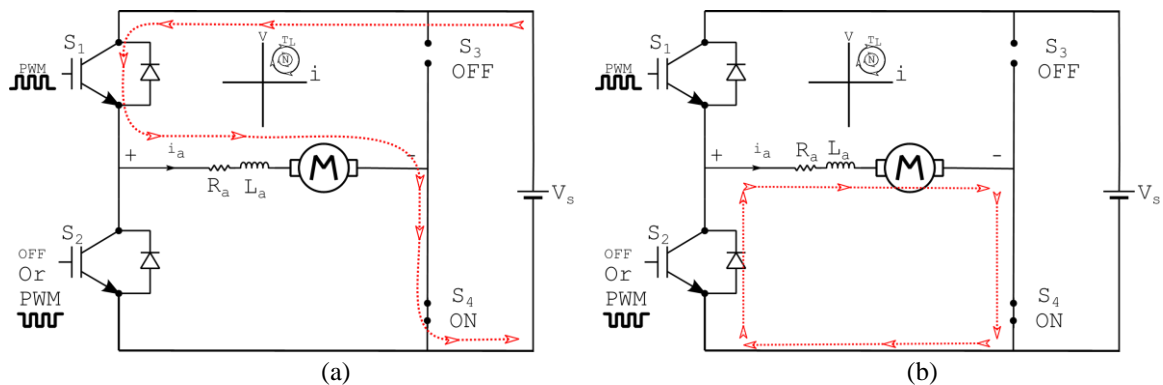


Figure 2. First quadrant operation (forward motoring mode): (a)  $S_1$  PWM is high and (b)  $S_1$  PWM is low

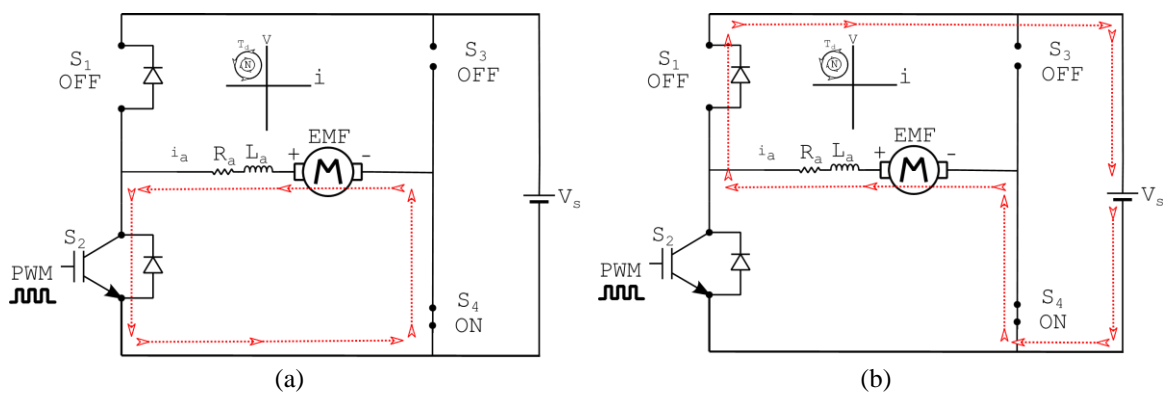


Figure 3. Second quadrant operation (forward regenerative braking): (a)  $S_2$  PWM is high and (b)  $S_2$  PWM is low

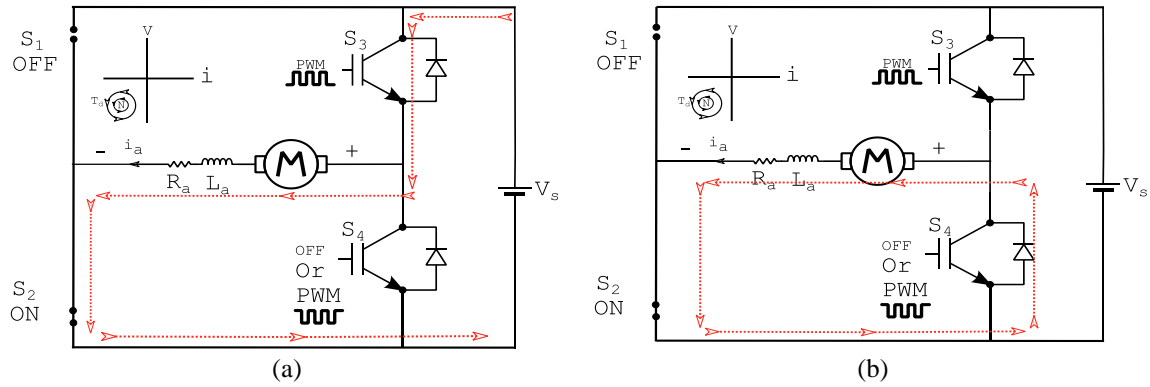


Figure 4. Third quadrant operation (reverse motoring mode): (a)  $S_3$  PWM is high and (b)  $S_3$  PWM is low

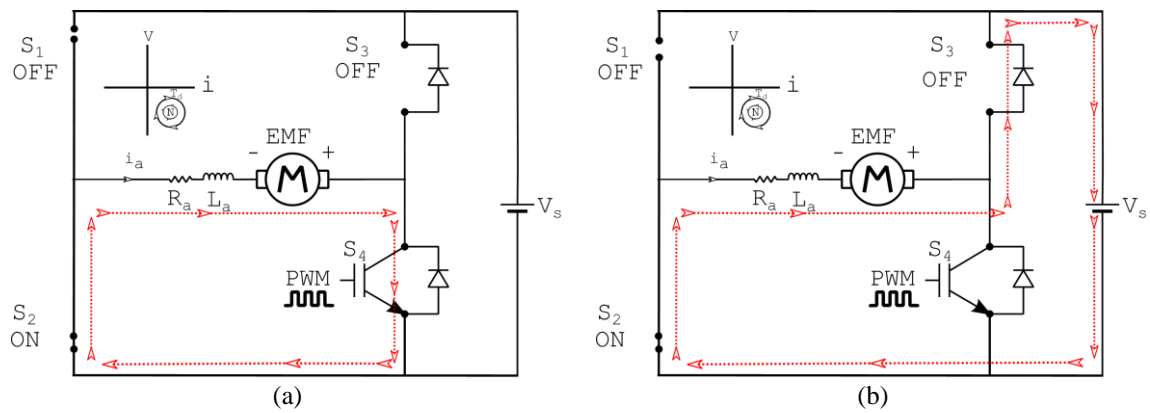


Figure 5. Fourth quadrant operation (reverse regenerative braking): (a)  $S_4$  PWM is high and (b)  $S_4$  PWM is low

## 2.2. Regenerative braking analysis

Regenerative braking is a system that allows an electric or hybrid vehicle to recover kinetic energy as it slows down and use it to recharge the battery [30], [31]. The regenerative braking mechanism will activate whenever the driver lifts their foot from the accelerator, causing the car to decelerate and the kinetic energy to return to the battery. The generated EMF shown in Figure 6 depends on the speed of the electric vehicle during the braking mode. As shown in Figure 6, during the time period from 0 to  $t_{on}$ , the energy stored in the vehicle's inertia is transferred to the armature coil of the motor  $L_a$ . From the time period  $t_{on}$  to  $T$ , the coil energy is transferred to the battery.

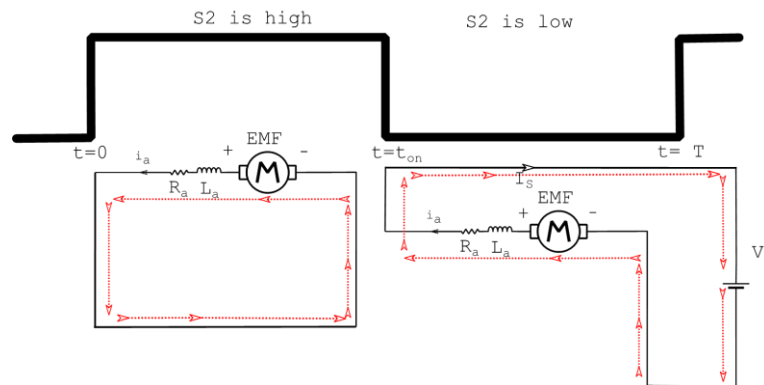


Figure 6. Regenerative braking operation in the second quadrant

The equation for the armature current from 0 to  $t_{on}$  of Figure 6 is shown in (1), and the equation for the same current from 0 to T is shown in (2) [32]-[35].

$$E - i_a R_a - L_a \frac{di_a}{dt} = 0 \quad (1)$$

$$E - i_a R_a - L_a \frac{di_a}{dt} = V_s \quad (2)$$

By solving (1), the armature current from 0 to  $t_{on}$  is shown in (3).

$$i_a = \frac{E}{R_a} + A_1 e^{-t/\tau} \quad \text{Where } \tau = \frac{L_a}{R_a} \quad (3)$$

And the armature current from  $t_{on}$  to T is shown in (4).

$$i_a = \frac{E - V_s}{R_a} + A_2 e^{-t/\tau} \quad (4)$$

The power fed to the supply i.e. regenerated power can be calculated using (5).

$$\text{Regenerative power } P_r(t) = V_s \times i_{a-\text{average}} = V_s \times \frac{1}{T} \int_{t_{on}}^T i_a dt \quad (5)$$

The regenerative power curve is shown in Figure 7, this power varies instantaneously with time, and the regeneration starts at time  $t_1$  and ends at time  $t_2$ , so the regenerative energy can be find using (6).

$$\text{Regenerative Energy} = \int_{t_1}^{t_2} P_r(t) dt \quad (6)$$

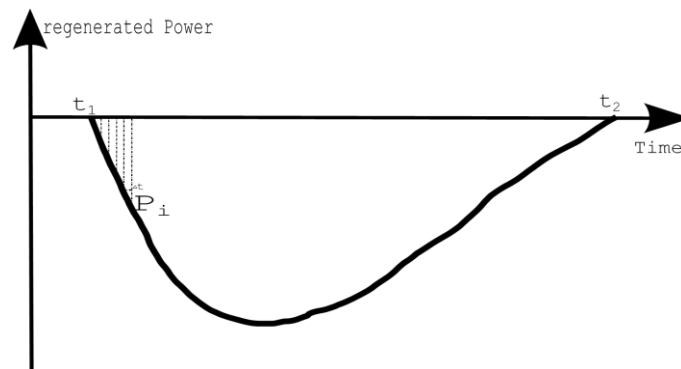


Figure 7. Regenerated power during the braking

### 3. RESULTS

The complete block diagram of the simulated system is shown in Figure 8. A microcontroller is used to control the entire system, allowing power to flow in both directions between the battery and the power converter. Table 1 shows the parameters used in the simulation and their justifications.

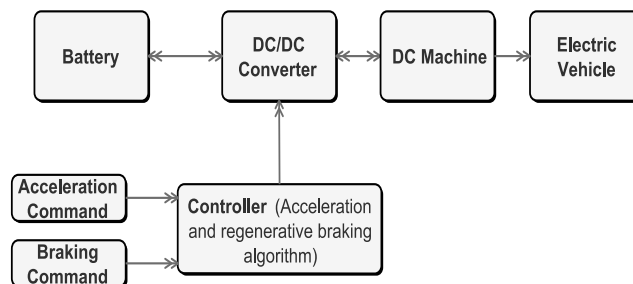


Figure 8. Block diagram for the proposed control system

Table 1. The parameters used in simulation

Parameter	Value	Unit	Justification
Motor power	5	HP	A standard motor power value used for small EV.
Load torque	10	Nm	A moderate load torque to simulate typical driving conditions.
Switching frequency (PWM)	1, 3, 5	kHz	Different frequencies are tested to assess the influence on regenerative braking efficiency.
Duty cycle (motoring mode)	90	%	This high duty cycle ensures maximum motor speed during motoring mode for performance testing.
Duty cycle (regenerative mode)	55-65	%	The optimal range for maximum energy recovery.
Simulation time	1	s	A short time interval that allows clear observation of the transitions between motoring and braking modes.
Regenerative energy	400	J	Maximum recovered energy during braking cycles, confirming system efficiency.

### 3.1. 4-quadrant chopper simulations

The implemented model of the 4-quadrant chopper is simulated in Simulink, as shown in Figure 9. The first quadrant operation is achieved by applying a PWM signal to the gate of transistor  $S_1$  and the complement signal to the gate of transistor  $S_2$ . Figure 10 provides an outline of the simulated model for forward motoring and forward regenerative braking. The general pulse generators are configured with 5 kHz switching frequency and its duty ration can be adjustable.

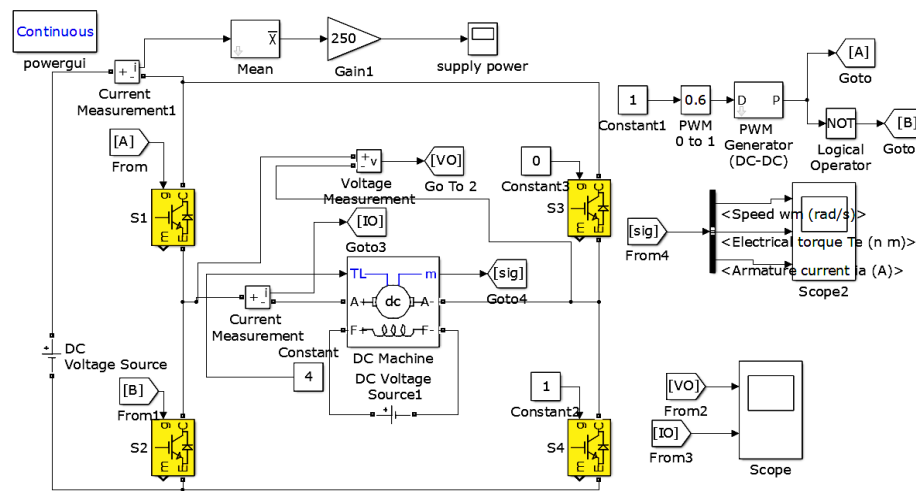


Figure 9. Simulink model for forward motoring mode

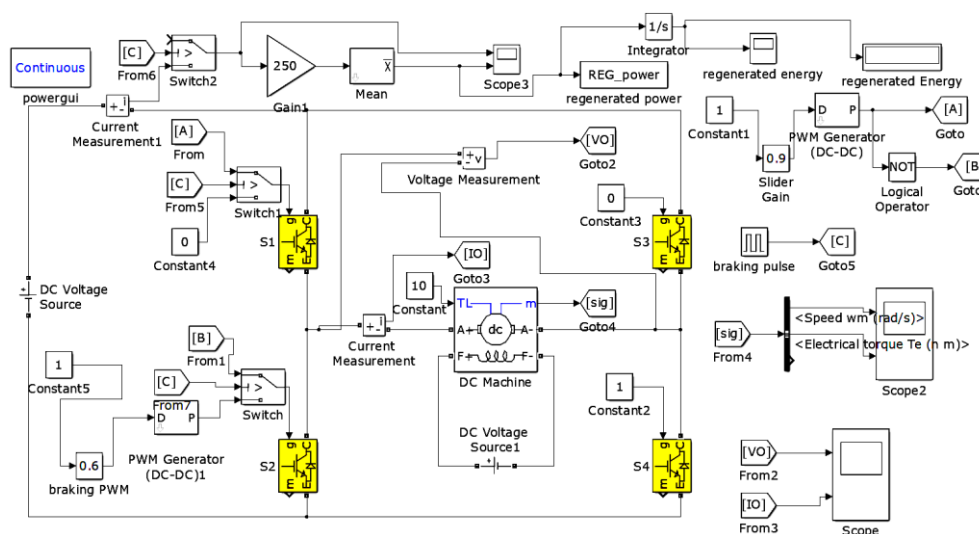


Figure 10. Simulink model for forward motoring and forward regenerative braking modes

The simulation time is 1 second, with 0.5 seconds for forward operation mode and 0.5 seconds for forward regenerative operation mode. As shown in Figure 10, a pulse generator (braking pulse) is configured with a period of 1 second and a pulse width of 50%. The ON time of the pulse operates the motor in forward motoring mode, while the OFF time operates the motor in reverse regenerative braking mode. During regenerative braking, a PWM signal is applied to transistor  $S_2$  (braking PWM), and keeping the upper transistor  $S_1$  OFF. The duty cycle and frequency can be adjusted to achieve the maximum regenerative braking energy, which results in a highly efficient braking system.

The motor is loaded with 10 N-m, when the braking sequence is initiated after 0.5 seconds, the speed gradually drops as shown in Figure 11(a), The negative electrical torque indicates the motor is in regenerative braking mode as shown in Figure 11(b), and the regenerative energy is rising as shown in Figure 12. Figure 13 shows the simulation results for a 5 hp DC motor with a constant load of 10 Nm applied to its shaft. The duty cycle for the motoring mode was set to 90%, while the duty cycle for regenerative braking varied from 5% to 95%. Different frequencies were applied during regenerative braking, like 1 kHz, 3 kHz, and 5 kHz. It was found that the maximum regenerative braking occurs at duty cycles between 55% to 65%.

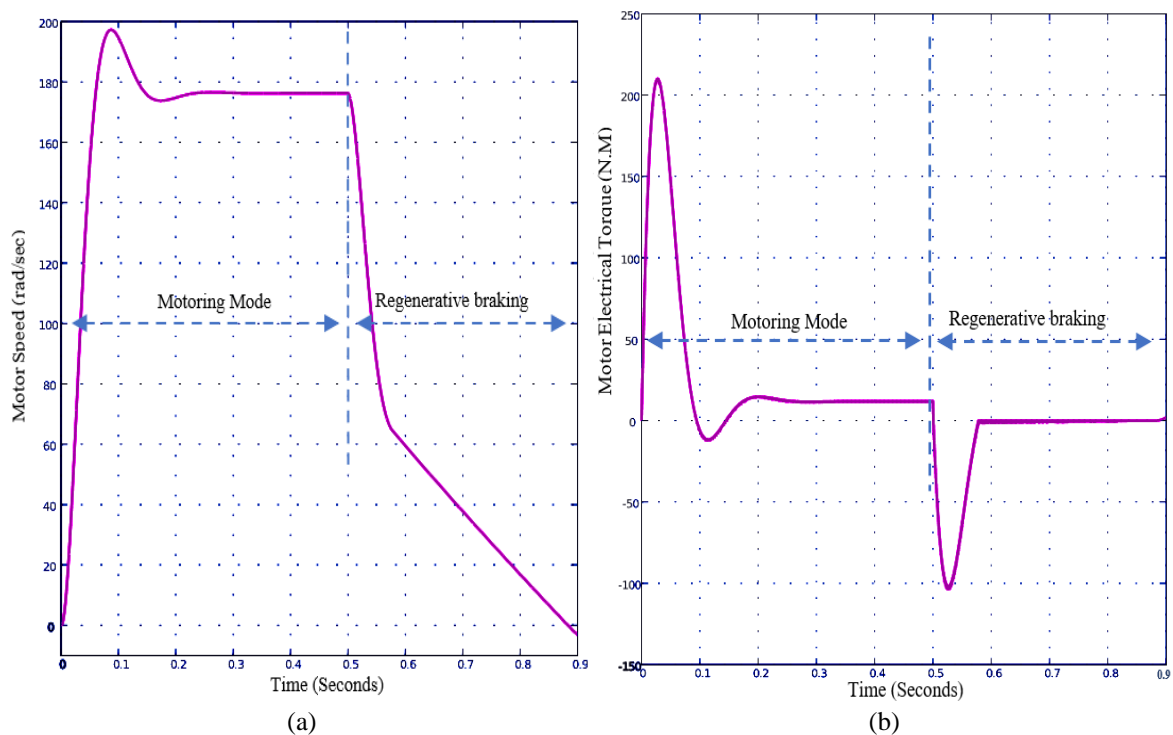


Figure 11. Motoring and regenerative braking modes: (a) motor speed and (b) motor electrical torque

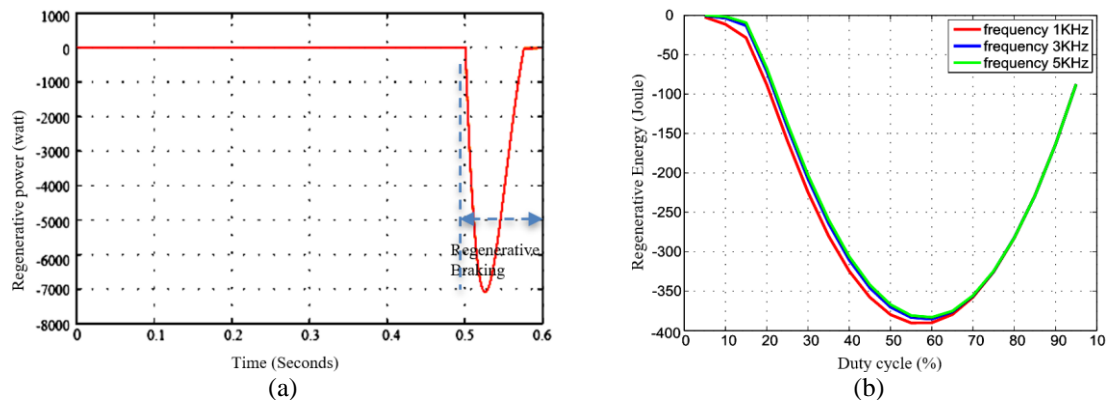


Figure 12. Regenerative braking power

Figure 13. Regenerative energy at different duty cycles and frequencies



### 3.2. Hardware implementation

The components of the complete system are shown in Figure 14(a). The hardware consists of a 4-quadrant chopper with four MOSFETs, each with a heat sink for cooling the heat generated in each switch. A microcontroller (PIC18F4431) generates the four gate signals required to run the four MOSFETs and manage the complete system. A dead time of 2 microseconds is considered between the upper and lower MOSFETs on the same chopper leg. 4 drivers TLP250 are used for isolating and scaling the gate signals generated by the microcontroller. A low power DC supply is used to energize the microcontroller with 5 V and 18 V for drivers.

A 1 hp, 24 V permanent magnet DC motor is used, along with a pedal accelerator that generates an analog signal from 0 to 5 V for generating a PWM signal according to the required speed. A forward-reverse switch is used to change between the forward and reverse motoring modes, and a regenerative braking push button is also included. The complete hardware components are shown in Figure 14(b), the proposed control system is used to drive the small car sample shown in Figure 15, regenerative braking enabled whenever the driver lifts their foot from the pedal accelerator.

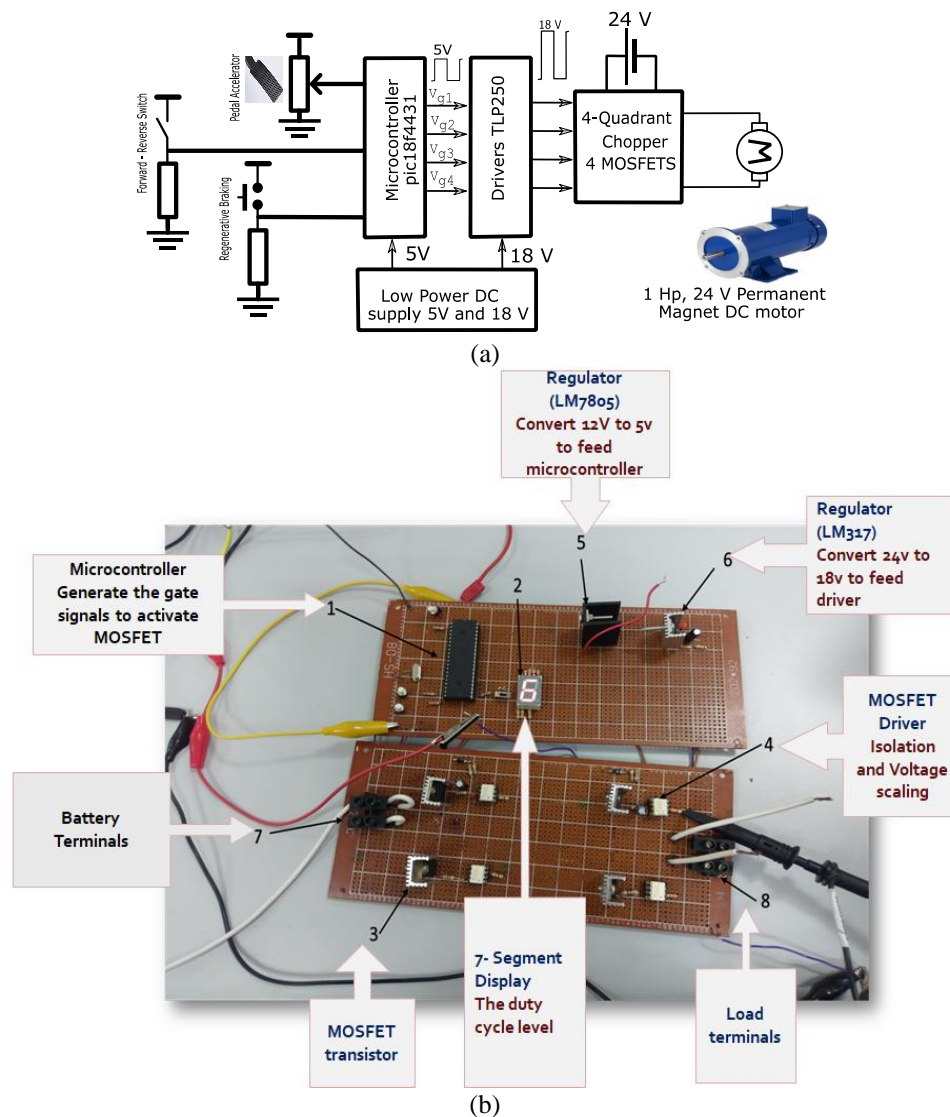


Figure 14. Experimental output voltage waveforms at different duty cycles: (a) schematic diagram and (b) hardware components

### 3.3. Experimental observations

The applied motoring mode PWM with a frequency of 4 kHz has been studied at different duty cycles; experimental waveforms for the output voltage are shown in Figure 16. Figure 16(a), shows the output voltage



at duty cycle 10%, while Figure 16(b) shows the output voltage at duty cycle 70%. Regenerative braking studied at different frequencies such as 1 kHz, 3 kHz, and 5 kHz. The braking PWM is applied on the lower MOSFETs. It has been found that the regenerative braking energy can reach up to 400 joules for each braking cycle for the used vehicle system. During experiment, it is observed that maximum regenerative energy in the range of 55 to 65 % of the duty cycle. The change in frequency has very less effect on the amount of regenerative energy.



Figure 15. Electric vehicle sample

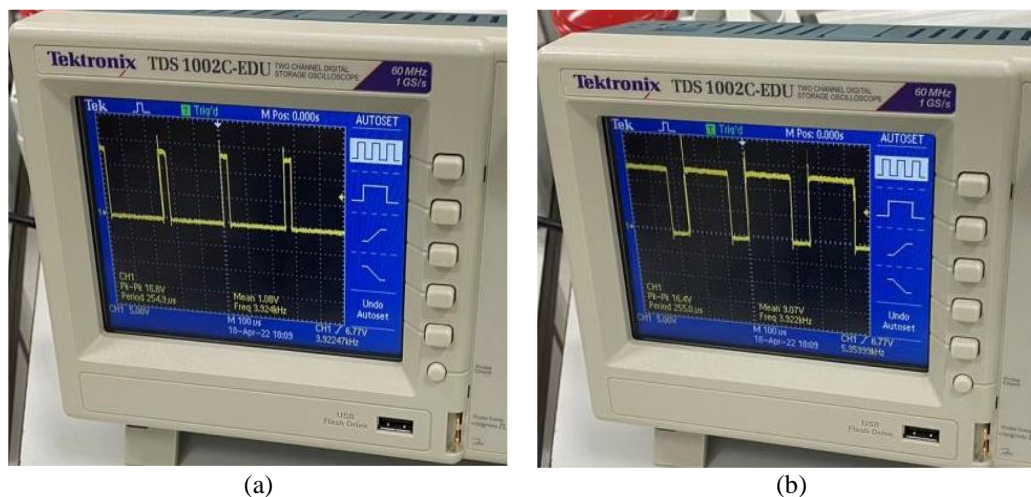


Figure 16. Experimental output voltage waveforms at different duty cycles: (a) 10% duty cycle and (b) 70% duty cycle

#### 4. CONCLUSION

Due to the fluctuating prices of gasoline and its negative impacts, switching to electric vehicles is considered as the need of the hour. A complete driving system for electric vehicles has been implemented. The regenerative braking could be able to save the energy stored in the battery thereby optimizing the safe running distance per battery charge to the extent of 5-10%. The maximum regenerated energy occurred at duty cycles between 55% and 65%. The designed driving system is used for driving a small real electric vehicle and has given acceptable results. The regenerated energy released around 400 joules of energy for every braking period in the proposed driving system and is based on vivid factors such as the speed of the electric vehicle, the system inertia, and the applied braking PWM duty cycle. The incorporation of regenerative braking not only conserved battery charge but also reduced reliance on mechanical braking systems thereby improving overall energy efficiency and sustainability in EV applications. This design was meant for a small car prototype; however, it can be further extended for the integration of large EVs.

## ACKNOWLEDGEMENTS

The research leading to these results has received funding from the Ministry of Higher Education, Research and Innovation (MoHERI) of the sultanate of Oman under the Block Funding Program. MoHERI Block Funding Agreement No MoHERI/BFP/UoTAS/01/2021.




## REFERENCES

- [1] G. Bieker, "A global comparison of the life-cycle greenhouse gas emissions of combustion engine and electric passenger cars," *Communications*, vol. 49, no. 30, pp. 847129–102, 2021.
- [2] N. Hill *et al.*, "Determining the environmental impacts of conventional and alternatively fuelled vehicles through LCA," 2020. doi: 10.2834/91418.
- [3] J. Fan, X. Meng, J. Tian, C. Xing, C. Wang, and J. Wood, "A review of transportation carbon emissions research using bibliometric analyses," *Journal of Traffic and Transportation Engineering*, vol. 10, no. 5, pp. 878–899, 2023, doi: 10.1016/j.jtte.2023.09.002.
- [4] N. A. Grigore and C. V. Kifor, "Are electric vehicles eco-friendly products? A review from life cycle and sustainability perspective," *MATEC Web of Conferences*, vol. 343, p. 07002, Aug. 2021, doi: 10.1051/mateconf/202134307002.
- [5] O.-O. Aderibigbe and T. Gumbo, "The role of electric vehicles in greening the environment: prospects and challenges," *REAL CORP 2023 Proceedings/Tagungsband 18-20 September 2023*, pp. 777–786, 2023.
- [6] D. Sun, F. Kyere, A. K. Sampene, D. Asante, and N. Y. G. Kumah, "An investigation on the role of electric vehicles in alleviating environmental pollution: evidence from five leading economies," *Environmental Science and Pollution Research*, vol. 30, no. 7, pp. 18244–18259, Oct. 2022, doi: 10.1007/s11356-022-23386-x.
- [7] M. Mruzek, I. Gajdač, L. Kučera, and T. Gajdošík, "The possibilities of increasing the electric vehicle range," *Procedia Engineering*, vol. 192, pp. 621–625, 2017, doi: 10.1016/j.proeng.2017.06.107.
- [8] I. Gajdač, L. Kučera, T. Gajdošík, and V. Konstantova, "A review of the factors and input parameters influencing the range of an Edison electric vehicle according to measurements," *Scientific Review Engineering and Environmental Sciences (SREES)*, vol. 31, no. 4, pp. 270–282, 2022.
- [9] I. Miri, A. Fotouhi, and N. Ewin, "Electric vehicle energy consumption modelling and estimation-A case study," *International Journal of Energy Research*, vol. 45, no. 1, pp. 501–520, Jan. 2021, doi: 10.1002/er.5700.
- [10] D. M. U and B. G. R., "A novel switching scheme for regenerative braking and battery charging for BLDC motor drive used in electric vehicle," in *2020 IEEE International Power and Renewable Energy Conference*, IEEE, Oct. 2020, pp. 1–6. doi: 10.1109/IPRECON49514.2020.9315226.
- [11] A. J. S. Renius, K. V. Kumar, A. A. Fredderics, and B. R. Guru, "Analysis of variable speed PFC chopper fed BLDC motor drive," *ARNP Journal of Engineering and Applied Sciences*, vol. 9, no. 12, pp. 2521–2527, 2014.
- [12] H. Mohan and R. K. P., "Modeling and control of DC chopper fed brushless DC motor," *International Research Journal of Engineering and Technology (IRJET)*, vol. 02, no. 03, pp. 1987–1994, 2015.
- [13] Z. S. Al-Sagar, M. S. Saleh, K. G. Mohammed, and A. Z. Sameen, "Modelling and simulation speed control of DC motor using PSIM," *IOP Conference Series: Materials Science and Engineering*, vol. 745, no. 1, p. 012024, Feb. 2020, doi: 10.1088/1757-899X/745/1/012024.
- [14] V. S. Patil, S. Angadi, and A. B. Raju, "Four quadrant close loop speed control of DC motor," in *2016 International Conference on Circuits, Controls, Communications and Computing (I4C)*, IEEE, Oct. 2016, pp. 1–6. doi: 10.1109/CIMCA.2016.8053305.
- [15] S. J. Rubavathy *et al.*, "Machine learning strategy for solar energy optimisation in distributed systems," *Energy Reports*, vol. 8, pp. 872–881, Nov. 2022, doi: 10.1016/j.egy.2022.09.209.
- [16] F. Alanazi, "Electric vehicles: Benefits, challenges, and potential solutions for widespread adaptation," *Applied Sciences*, vol. 13, no. 10, p. 6016, May 2023, doi: 10.3390/app13106016.
- [17] P. V. S. Aditya and S. J. Rubavathy, "VSI controller integrated DC-DC converter for electrical vehicle charging system in PV solar grid," *Electric Power Components and Systems*, pp. 1–14, Nov. 2023, doi: 10.1080/15325008.2023.2270593.
- [18] W. Li *et al.*, "Regenerative braking control strategy for pure electric vehicles based on fuzzy neural network," *Ain Shams Engineering Journal*, vol. 15, no. 2, p. 102430, Feb. 2024, doi: 10.1016/j.asej.2023.102430.
- [19] Y. Zhang, Y. Zhang, Z. Ai, Y. L. Murphey, and J. Zhang, "Energy optimal control of motor drive system for extending ranges of electric vehicles," *IEEE Transactions on Industrial Electronics*, vol. 68, no. 2, pp. 1728–1738, Feb. 2021, doi: 10.1109/TIE.2019.2947841.
- [20] S. Jung and J. Ko, "Study on regenerative energy recovery of electric vehicle through voltage control using switched capacitor," *IEEE Transactions on Vehicular Technology*, vol. 70, no. 5, pp. 4324–4339, May 2021, doi: 10.1109/TVT.2021.3073148.
- [21] A. A. E. B. A. El Halim, E. H. E. Bayoumi, W. El-Khattam, and A. M. Ibrahim, "Electric vehicles: a review of their components and technologies," *International Journal of Power Electronics and Drive Systems (IJPEDS)*, vol. 13, no. 4, pp. 2041–2061, Dec. 2022, doi: 10.11591/ijpeds.v13.i4.pp2041-2061.
- [22] S. Yu, J. Zhang, and L. Wang, "Power management strategy with regenerative braking for fuel cell hybrid electric vehicle," in *2009 Asia-Pacific Power and Energy Engineering Conference*, IEEE, Mar. 2009, pp. 1–4. doi: 10.1109/APPEEC.2009.4918610.
- [23] S. Heydari, P. Fajri, M. Rasheduzzaman, and R. Sabzehgar, "Maximizing regenerative braking energy recovery of electric vehicles through dynamic low-speed cutoff point detection," *IEEE Transactions on Transportation Electrification*, vol. 5, no. 1, pp. 262–270, Mar. 2019, doi: 10.1109/TTE.2019.2894942.
- [24] W. Yeo, S. Jung, S. Kim, K. Park, and J. Ko, "A regenerative energy recovery system for electric vehicles charging a battery at a low speed," *Advances in Science, Technology and Engineering Systems Journal*, vol. 5, pp. 64–73, 2020.
- [25] S. Heydari, P. Fajri, R. Sabzehgar, and A. Asrari, "Optimal brake allocation in electric vehicles for maximizing energy harvesting during braking," *IEEE Transactions on Energy Conversion*, vol. 35, no. 4, pp. 1806–1814, Dec. 2020, doi: 10.1109/TEC.2020.2994520.
- [26] S. Bouradi, K. Negadi, R. Araria, B. Boumediene, and M. Koulali, "Design and implementation of a four-quadrant DC-DC converter based adaptive fuzzy control for electric vehicle application," *Mathematical Modelling of Engineering Problems*, vol. 9, no. 3, pp. 721–730, Jun. 2022, doi: 10.18280/mmep.090319.
- [27] R. Shrivastava, P. Shrivastava, M. Sawale, and M. Gupta, "Design and implementation of four quadrant DC drive using class E chopper," *International Research Journal of Engineering and Technology (IRJET)*, vol. 07, no. 08, pp. 1959–1963, 2020.
- [28] R. Sonbarse, A. Ringe, and A. A. Bhalerao, "MATLAB simulation on speed control of four quadrant DC drive using chopper," *International Research Journal of Engineering and Technology (IRJET)*, vol. 04, no. 3, pp. 502–504, 2017.


- [29] B. N. Krishna, B. Nagaraju, and P. V. Kumar, "Design and implementation of four quadrant DC drive using chopper," in *2015 International Conference on Electrical, Electronics, Signals, Communication and Optimization (EESCO)*, IEEE, Jan. 2015, pp. 1–5. doi: 10.1109/EESCO.2015.7253726.
- [30] Z. Ding, D. Zhao, and J. Zuo, "Modeling and simulation about an electric car's regenerative braking system," in *2007 International Conference on Mechatronics and Automation*, IEEE, Aug. 2007, pp. 1705–1709. doi: 10.1109/ICMA.2007.4303807.
- [31] V. Vodovozov, Z. Raud, and E. Petlenkov, "Review on braking energy management in electric vehicles," *Energies*, vol. 14, no. 15, p. 4477, Jul. 2021, doi: 10.3390/en14154477.
- [32] M. H. Rashid, *Power electronics: Circuits, devices, and application*. 2011.
- [33] R. Ayyanar and N. Mohan, "Novel soft-switching DC-DC converter with full ZVS-range and reduced filter requirement. I. Regulated-output applications," *IEEE Transactions on Power Electronics*, vol. 16, no. 2, pp. 184–192, Mar. 2001, doi: 10.1109/63.911142.
- [34] B. K. Bose, "Power electronics and motor drives recent progress and perspective," *IEEE Transactions on Industrial Electronics*, vol. 56, no. 2, pp. 581–588, Feb. 2009, doi: 10.1109/TIE.2008.2002726.
- [35] D. R. Yengalwar, S. S. Zade, and D. L. Mute, "Four quadrant speed control of DC motor using chopper," *International Journal of Engineering Sciences & Research Technology (IJESRT)*, vol. 4, no. 2, pp. 401–406, 2015.

## BIOGRAPHIES OF AUTHORS






**Magdy Saoudi Abdelfatah**    is an assistant professor at the Department of Electrical Engineering, University of Technology and Applied Sciences, Suhar, Sultanate of Oman. He received his B.Eng. in Electrical Power and Machines Engineering from Zagazig University, Egypt in 2004, and his M.Eng. and Ph.D. in Power Electronics from Zaragoza University, Spain in 2012. His research interests in the field of power electronics applications, including the complete design and analysis of power converters, motor drives, and renewable energy. He can be contacted at email: magdy.saoudi@utas.edu.om.



**Parmal Singh Solanki**    is an assistant professor at the Department of Electrical Engineering, University of Technology and Applied Sciences, Suhar, Sultanate of Oman. He received his B.Eng. in Electrical Engineering from University of Poona, India in 1992, and his M.Eng. in Power System from University of Rajasthan, India in 2001 while Ph.D. in Demand Side Management of Electrical Power from Glasgow Caledonian University, Scotland (UK) in 2012. His research interests in the field of power system, including the condition monitoring, regulation of electrical energy, and micro grid applications using distributed generation. He can be contacted at email: parmal.solanki@utas.edu.om.



**Sasidharan Sreedharan**    is an assistant professor at the Department of Electrical Engineering, University of Technology and Applied Sciences, Suhar, Sultanate of Oman. He received his B.Tech. and M.Tech. from Govt Engineering Thrissur, Kerala, India in 1995 and 1998 respectively. He received his Doctorate from The Asian Institute of Technology, Bangkok in 2010 while the Post-Doctoral Research Fellowship from RED Lab, Renewable Energy Design Laboratory, University of Hawaii, Manoa, USA in 2015. His research interests are in high performance computing, big data analytics, and smart computing frame work applied to smart grid, and distributed generation in microgrid. He can be contacted at email: sasidharan.sreedarsan@utas.edu.om.